

Prediction of direct band gaps in monolayer (001) and (111)GaAs/GaP superlattices

Robert G. Dandrea and Alex Zunger

Citation: *Applied Physics Letters* **57**, 1031 (1990); doi: 10.1063/1.103556

View online: <http://dx.doi.org/10.1063/1.103556>

View Table of Contents: <http://scitation.aip.org/content/aip/journal/apl/57/10?ver=pdfcov>

Published by the [AIP Publishing](#)

Articles you may be interested in

[Role of structural and chemical contributions to valence-band offsets at strained-layer heterojunctions: The GaAs/GaP \(001\) case](#)

J. Vac. Sci. Technol. B **14**, 2936 (1996); 10.1116/1.588937

[GaAs/GaP strained-layer superlattices grown by atomic layer epitaxy](#)

J. Vac. Sci. Technol. B **8**, 741 (1990); 10.1116/1.585003

[Optical properties of GaAs/GaP strained-layer superlattices](#)

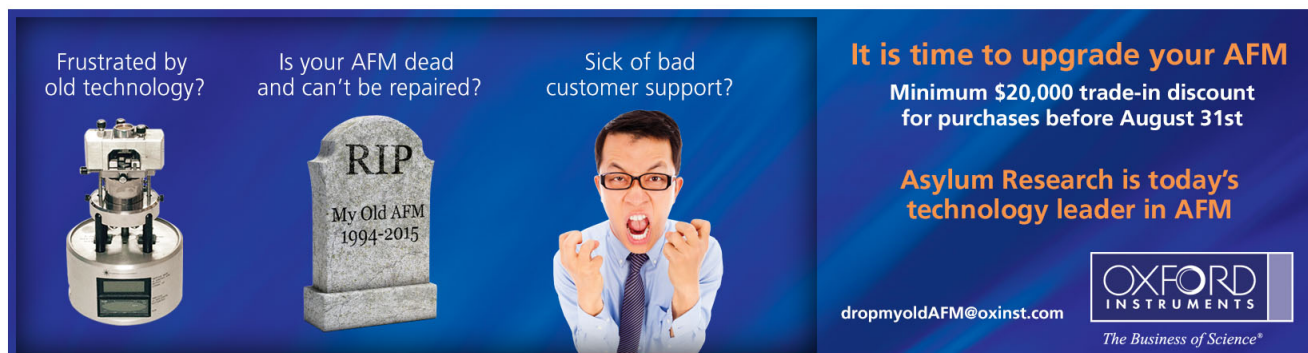
J. Appl. Phys. **67**, 2044 (1990); 10.1063/1.345588

[Ellipsometric study of GaAs/GaP superlattices](#)

Appl. Phys. Lett. **56**, 358 (1990); 10.1063/1.102784

[\(111\) oriented \(GaAs\) n \(AlAs\) n superlattices are direct band-gap materials for all n's](#)

Appl. Phys. Lett. **53**, 2077 (1988); 10.1063/1.100415

An advertisement for Oxford Instruments' Asylum Research AFM. The background is dark blue with a light blue wave pattern. On the left, there are three panels: 1) A photograph of an AFM with the text 'Frustrated by old technology?'. 2) A tombstone with 'RIP' and 'My Old AFM 1994-2015' with the text 'Is your AFM dead and can't be repaired?'. 3) A man in a suit shouting with the text 'Sick of bad customer support?'. On the right, there is a large white box with the text 'It is time to upgrade your AFM', 'Minimum \$20,000 trade-in discount for purchases before August 31st', and 'Asylum Research is today's technology leader in AFM'. At the bottom right, the Oxford Instruments logo is shown with the tagline 'The Business of Science®' and the email address 'dropmyoldAFM@oxinst.com'.

Prediction of direct band gaps in monolayer (001) and (111) GaAs/GaP superlattices

Robert G. Dandrea and Alex Zunger
Solar Energy Research Institute, Golden, Colorado 80401

(Received 26 March 1990; accepted for publication 19 June 1990)

The bulk GaAs_{0.5}P_{0.5} alloy with lattice constant $a(0.5)$ has an indirect band gap. First-principles self-consistent pseudopotential band structure calculations show that the monolayer (GaAs)₁(GaP)₁ superlattice (SL) in either the (001) or the (111) layer orientation Γ is also indirect if constrained epitaxially on a substrate whose lattice constant is $a(0.5)$. However, if grown coherently on a GaAs substrate we predict that both of these SLs will have a direct band gap. This is explained in terms of the deformation potentials of the underlying materials. Predicted band offsets are given for both (001) and (111) GaP/GaAs.

GaAs/GaAsP superlattices (SLs) were among the first semiconductor superstructures to be grown.^{1,2} More recently, *coherent* (001) oriented (GaAs)_{1...x}(P_x)_p (GaP)_q SLs were obtained with $p, q \sim 20$ monolayers on lattice-matched (graded) substrates.³ Tight-binding and effective mass calculations⁴ proposed that such SLs have a "pseudo-direct" band gap (folded from X_{1c}) attributed to the observed SL photoluminescence.³ Very recently, however, the ultimate limit of coherent ultrathin (GaAs)_p(GaP)_q SLs with $p, q \sim 1-6$ monolayers was achieved both through layer-by-layer deposition using atomic layer molecular beam epitaxy⁵ [(001) ordering], as well as by spontaneous ordering of a homogeneous GaAs_{1-x}P_x alloy seen in vapor deposition growth^{6,7} [(111) ordering, $p = q = 1$]. The electronic structure of these monolayer SLs is still unexplored, either experimentally or theoretically. At this limit, where conventional effective mass and envelope function descriptions are no longer valid, direct band-structure calculations (treating the SL as a periodic crystal in its own right^{8,9}) are needed. Using self-consistent nonlocal pseudopotential band theory¹⁰ we show (Fig. 1) that whereas on a substrate having the lattice constant $a_s = \bar{a}$ of the GaAs_{0.5}P_{0.5} alloy, both the (001) and (111) monolayer ($p = q = 1$) superlattices have an indirect gap, on the GaAs substrate $a_s = a_{\text{GaAs}}$, both SLs are predicted to have a direct band gap.

We use the local density approximation as implemented by the plane wave nonlocal pseudopotential method,¹⁰ a large basis set consisting of all plane waves with kinetic energies up to 15 Ry (~ 550 basis functions) and the SL equivalent of ten special zinc blende k points for Brillouin zone integration.¹¹ Since we model a *coherent* SL, we fix the lattice parameter parallel to the substrate at a_s and optimize all other structural parameters (including the cell-internal atomic positions) to reach a minimum of the total energy. Valence-band offsets are predicted [values given in Figs. 2(b), 2(c)] by calculations on $p = q = 3$ SLs. We do not use tight-binding³ or effective mass³⁻⁵ methods, nor do we input empirical deformation potentials; the virtual crystal approximation (VCA) calculation described below is used only to *analyze* the results, not to obtain them. The local density approximation (LDA) used

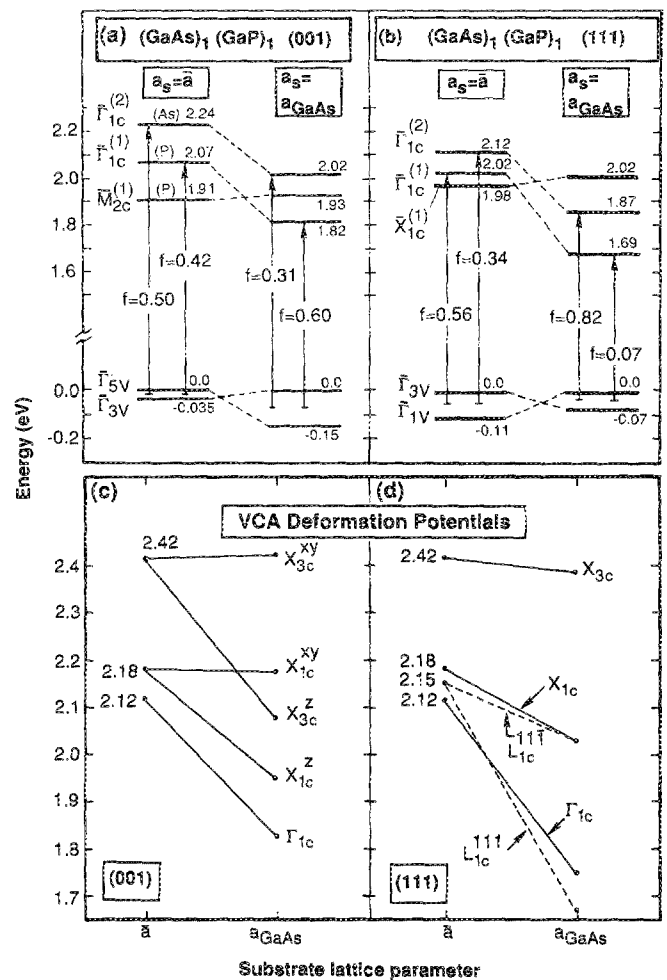


FIG. 1. Calculated energy levels for the monolayer (GaAs)₁(GaP)₁ SLs in: (a) (001) orientation and (b) (111) orientation on two different substrates a_s . The LDA calculated conduction bands were rigidly shifted upwards by 0.75 eV. Valence energies here are without spin-orbit splitting, consideration of which (within a quasi-cubic model¹²) decreases all gaps 0.04–0.07 eV. f is the square of the momentum matrix element (summed over the three valence maxima at Γ), in Ry. In (c) and (d) we show the respective biaxial deformation potentials for VCA Ga(AsP). Note how increasing a_s from \bar{a} to a_{GaAs} leads to an indirect-to-direct crossover.

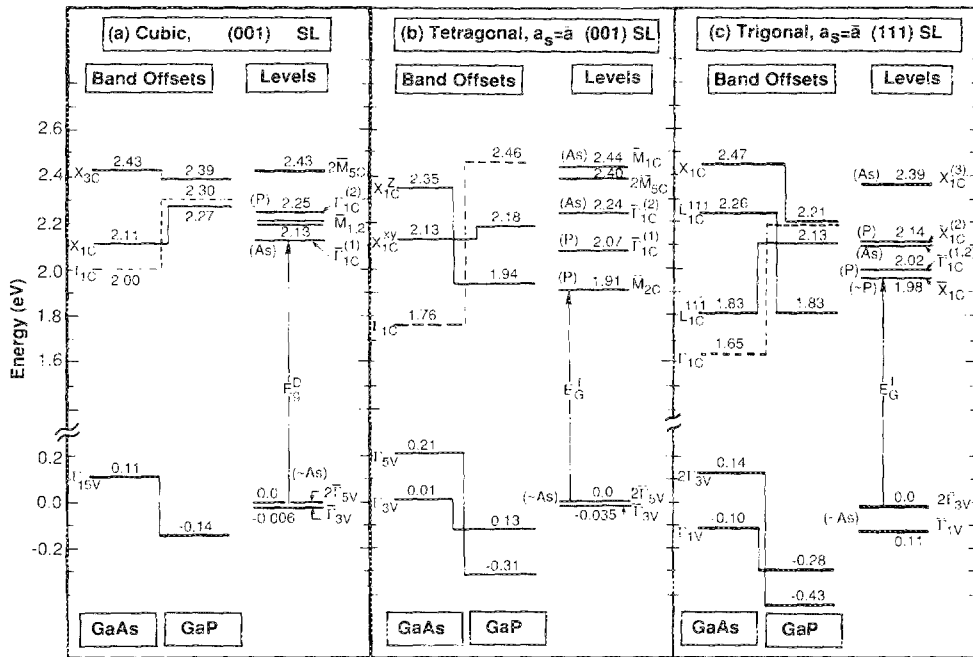


FIG. 2. Calculated band offsets (for thick GaP/GaAs) and SL energy levels [for $(\text{GaAs})_1(\text{GaP})_1$] on $a_s = \bar{a}$: (a) cubic (001) SL, (b) (001) SL with cell internal tetragonal relaxations, and (c) (111) SL with cell internal trigonal relaxations. The labels P and As denote the atom on which localization is largest. Conduction-band levels were shifted upwards by 0.75 eV.

here underestimates band gaps; we have hence rigidly shifted our calculated conduction bands upwards by the average LDA versus experimental error for GaP and GaAs (0.75 eV). Consideration of the remaining 0.1 eV error in conduction-band energies does not, however, affect our major conclusions regarding a direct-to-indirect transition.

Our calculations give most reliably the valence-band offsets [Figs. 2(b)–2(c), without spin-orbit splittings], which are unaffected by the above conduction-band error. Including both strain and spin-orbit¹² splitting, we calculate a valence offset between the spin-orbit split of $\Gamma_{5V}(\text{As})-\Gamma_{3V}(\text{P})$ for (001) of 0.44 eV, and between $\Gamma_{3V}(\text{As})-\Gamma_{1V}(\text{P})$ for (111) of 0.52 eV. We find [Figs. 1(a), 1(b)] that for $a_s = \bar{a}$ the SLs have an *indirect* band gap for both the (001) and the (111) orientations with conduction-band minima (CBM) at the \bar{M}_{2C} and \bar{X}_{1C} SL states, respectively. However, for $a_s = a_{\text{GaAs}}$ both SLs are predicted to have *direct band gaps* [including spin-orbit¹² effects, at 1.78 eV (700 nm) and 1.64 eV (760 nm) for (001) and (111), respectively] with substantial transition probabilities [denoted “*f*” in Figs. 1(a), 1(b)] from the valence-band maximum (VBM). In what follows we analyze these results in terms of a simple model which reveals the underlying physics of direct versus indirect gaps in these SLs.

In these short-period SLs, it is most natural to think of SL states as evolving from the states of a virtual crystal approximation (VCA) binary $\text{Ga}\langle\text{PAs}\rangle$ compound whose unit cell is commensurate with that of the SL. Figures 1(c) and 1(d) show the pseudopotential calculated VCA band-edge energies as a function of the lattice parameter a_s parallel to the substrate. In forming a SL on a given substrate, these VCA states are subjected to (i) folding into the SL Brillouin zone, as well as (ii) interactions between the folded states through the perturbing potential $\delta V = V_{\text{SL}} - V_{\text{VCA}}$ which can split and shift them. Since GaP and GaAs have a 3.7% lattice mismatch, the pertur-

bation changing the VCA into the SL can be broken into a chemical piece δV_{chem} (where the virtual $\langle\text{AsP}\rangle$ anion is changed to As and P in the respective halves of the SL) and a structural piece δV_{struc} (where the two halves of the SL relax to their equilibrium epitaxial layer spacings). As there are exactly two VCA $\text{Ga}\langle\text{AsP}\rangle$ unit cells in each SL cell, the SL *translational* symmetry requires that each of the SL states at wave vector $\bar{\mathbf{k}}$ be composed of (generally many) VCA states coming from just *two* \mathbf{k} points in the VCA Brillouin zone. Denoting SL states by an overbar, these folding relationships for the principal band extrema in the (001) SL are $\bar{\Gamma} = (2\pi/a)(0,0,0) \leftrightarrow \Gamma + \bar{X}^z$, $\bar{M} = (2\pi/a)(1,0,0) \leftrightarrow X^x + X^y$, and $\bar{R} = (2\pi/a)(\frac{1}{2}, \frac{1}{2}, \frac{1}{2}) \leftrightarrow L^{111} + L^{1\bar{1}\bar{1}}$; for the (111) SL they are $\bar{\Gamma} \leftrightarrow \Gamma + L^{111}$ and $\bar{X} = (2\pi/a)(001) \leftrightarrow X^z + L^{1\bar{1}\bar{1}}$. Note that (even without strain) the threefold degenerate X valley of zinc blende splits in the (001) SL into \bar{X}^z (which folds into $\bar{\Gamma}$) and $X^x + X^y$ (which fold into \bar{M}), while in the (111) SL the four L valleys split into L^{111} ($\bar{\Gamma}$ folding) and $L^{1\bar{1}\bar{1}}$ (folds to \bar{X}). Clearly the SL will be direct at $\bar{\Gamma}$ only if the $\bar{\Gamma}$ folding states are lower in energy than the non- $\bar{\Gamma}$ folding state. The SL point-group symmetry decides what type (i.e., representations) of VCA states are compatible with a given SL state. These compatibility relations depend both on the repeat period⁸ p and on whether the common atom in $(AC)_p(BC)_p$ is an anion or a cation (since X_1 and X_3 change their role⁹). Compatibility relations for the $p = 1$ common cation case (origin at the anion) are given in Table I. This table also gives (for $a_s = \bar{a}$) the projections of the VCA states onto the SL states. It shows that the perturbing potential δV is relatively weak, coupling only VCA states nearby in energy. In the following we demonstrate how controlling the relative energies of these low-lying VCA states through strain (appropriate to the epitaxial growth conditions) can change indirect gap $(\text{GaP})_1(\text{GaAs})_1$ SLs to direct.

Consider the case $a_s = \bar{a}$, where the pertinent VCA

TABLE I. Squared projections of SL wave functions for $a_s = \bar{a}$ onto those of zinc blende VCA. All energies ϵ (in eV) are with respect to the valence-band maximum (VBM). Here $L = L^{111}$ and $L' = L^{11\bar{1}}$. The SL states at the VBM have 99 and 96% of the VCA $\langle \Gamma_{15v} \rangle$ character for the (001) and (111) SLs, respectively.

SL states		VCA states			
$\bar{\epsilon}$	$\bar{\psi}$	$\langle \Gamma_{1c} \rangle$ $\epsilon = 2.12$	$\langle X_{1c} \rangle$ $\epsilon = 2.18$	$\langle X_{3c} \rangle$ $\epsilon = 2.42$	$\langle L_{1c} \rangle$ $\epsilon = 2.15$
(001):					
2.07	$\bar{\Gamma}_{1c}^{(1)}$	0.60	0.40 (z)	0	0
2.24	$\bar{\Gamma}_{1c}^{(2)}$	0.40	0.60 (z)	0	0
1.91	\bar{M}_{2c}	0	1.0(x,y)	0	0
2.40	\bar{M}_{5c}	0	0	1.0(x,y)	0
2.44	\bar{M}_{1c}	0	1.0(x,y)	0	0
2.09	\bar{R}_{3c}	0	0	0	1.0(L,L')
2.18	\bar{R}_{1c}	0	0	0	1.0(L,L')
(111):					
2.02	$\bar{\Gamma}_{1c}^{(1)}$	0.78	0	0	0.22 (L)
2.12	$\bar{\Gamma}_{1c}^{(2)}$	0.22	0	0	0.78 (L)
1.98	$\bar{X}_{1c}^{(1)}$	0	0.16 (z)	0.10 (z)	0.74 (L')
2.14	$\bar{X}_{1c}^{(2)}$	0	0.82 (z)	0.06 (z)	0.12 (L')
2.39	$\bar{X}_{1c}^{(3)}$	0	0.02 (z)	0.83 (z)	0.15 (L')

states (denoted by angular brackets) correspond to cubic materials with unsplit states [Figs. 1(c) and 1(d)]. Since the $\langle X_{3c} \rangle$ state is higher in energy [Fig. 1(c)], only the $\bar{\Gamma}_{1c}$ and $\bar{M}_{1,2}$ states occur near the CBM of an (001) SL. Turning on first the chemical perturbation $\delta V_{\text{chem}}(\mathbf{r})$ leaves the system cubic [Fig. 2(a)]; note that this does *not* correspond to any real system]. The nondegenerate $\langle \Gamma_{1c} \rangle$ and $\langle X_{1c}^z \rangle$ VCA states interact (in second order) producing the SL states $\bar{\Gamma}_{1c}^{(1)}$ and $\bar{\Gamma}_{1c}^{(2)}$ (As-like and P-like, respectively) while the VCA degenerate $\langle X_{1c}^{xy} \rangle$ states split (in first order) into the SL states \bar{M}_{1c} and \bar{M}_{2c} . The CBM is the $\bar{\Gamma}_{1c}^{(1)}$ state [Fig. 2(a)], hence the gap is *direct*. Although not shown, this occurs also in the cubic (111) SLs. Note that (AlAs)_p (GaAs)_p being lattice matched ($\delta V_{\text{str}} = 0$) was also predicted⁸ to have a direct gap in the (111) orientation.

This situation changes when we turn on the structural perturbation $\delta V_{\text{str}}(\mathbf{r})$ which causes tetragonal distortions of $c/a = 0.966$ and 1.034 in the GaP and GaAs halves, respectively. As seen in Fig. 2(b), these tetragonal deformations cause X^z - X^{xy} splittings of 0.22 and 0.24 eV, causing the $\bar{\Gamma}_{1c}^{(1)}$ state to change from 85% As localized to 85% P localized (due to the X_{1c}^z offset now being lower in the P half). Furthermore, the stronger perturbation causes a much larger splitting of $X_{1c}^z + X_{1c}^{xy}$ into \bar{M}_{1c} and \bar{M}_{2c} ; the relaxed SL is now *indirect* at \bar{M}_{2c} because of the large first-order matrix element $\langle X_{1c}^z | \delta V | X_{1c}^{xy} \rangle$. A similar situation occurs in the (111) SL on $a_s = \bar{a}$ [Fig. 2(c)] where the $L_{1c}^{11\bar{1}}$ -derived SL \bar{X}_{1c} state forms the CBM. Hence, both

(001) and (111) SLs on $a_s = \bar{a}$ are indirect because of δV_{str} .

This analysis reveals the way to produce a direct band gap SL. Since the structural perturbation alone converted the SLs on $a_s = \bar{a}$ to indirect [compare Fig. 2(a) with 2(b)], we need to structurally perturb those VCA states which form the indirect band edges [X_{1c}^{xy} for (001), $X^z + L^{11\bar{1}}$ for (111)] so that they are displaced to higher energies. The VCA deformation potentials of Figs. 1(c) and 1(d) show the way: increase the substrate lattice parameter a_s away from \bar{a} . The *negative* biaxial deformation potentials for these states increase their energies, whereas the $\bar{\Gamma}$ folding $\langle \Gamma_{1c} \rangle$, $\langle X_{1c}^z \rangle$, and $\langle L^{111} \rangle$ states, having positive biaxial deformation potentials, are lowered. Indeed, self-consistent SL calculations for $a_s = a_{\text{GaAs}}$ [Figs. 1(a), 1(b)] show that they are direct. [We have checked also the dispersion along Δ_{xy} for (001) and Δ_z for (111); the CBM is still at $\bar{\Gamma}$]. Examination of the calculated dipole matrix elements squared [denoted as f in Figs. 1(a), 1(b)] reveals that the (111) SL is "pseudodirect" (greater $\langle L_{1c} \rangle$ folded character than $\langle \Gamma_{1c} \rangle$ character, hence small f) while the (001) SL is strongly direct (large f). This is analogous to the situation we encountered in Si_nGe_n (001) superlattices¹³ being indirect on a Si substrate, but (quasi) direct on a substrate with a larger lattice parameter (e.g., Ge). The large biaxial deformation potentials of $\bar{\Gamma}$ folding states are a general feature of adamantine semiconductors, and should thus lead to a decrease in direct energy gaps with substrate lattice constant in other instances of coherent epitaxial growth. Experimental examination of the optical properties of monolayer GaAsP SLs on GaAs is called for.

¹ Zh. I. Alferov, Yu. V. Zhilav, and Yu. V. Schmartsev, *Sov. Phys. Semicond.* **5**, 174 (1971).

² J. W. Matthews and A. E. Blakeslee, *J. Cryst. Growth* **27**, 118 (1974); **32**, 265 (1976).

³ G. C. Osbourn, R. M. Biefield, and P. L. Gourley, *Appl. Phys. Lett.* **41**, 172 (1982).

⁴ G. C. Osbourn, *J. Vac. Sci. Technol.* **21**, 469 (1982).

⁵ G. Armelles, M. Recio, A. Ruiz, and F. Briones, *Solid State Commun.* **71**, 431 (1989); M. Recio, G. Armelles, J. Melendez, and Briones, *J. Appl. Phys.* **67**, 2044 (1990); G. Armelles, J. M. Rodriguez, and F. Briones, *Appl. Phys. Lett.* **56**, 358 (1990).

⁶ W. E. Plano, D. W. Nam, J. S. Major, K. C. Hsieh, and N. Holonyak, *Appl. Phys. Lett.* **53**, 2537 (1988).

⁷ H. R. Jen, D. S. Cao, and G. B. Stringfellow, *Appl. Phys. Lett.* **54**, 1890 (1989).

⁸ S. H. Wei and A. Zunger, *Appl. Phys. Lett.* **53**, 2077 (1988); *J. Appl. Phys.* **63**, 5794 (1988).

⁹ S. H. Wei and A. Zunger, *Appl. Phys. Lett.* **56**, 662 (1990); *Phys. Rev. B* **39**, 3279 (1989); J. E. Bernard, S. H. Wei, D. M. Wood, and A. Zunger, *Appl. Phys. Lett.* **52**, 311 (1988).

¹⁰ J. Ihm, Z. Zunger, and M. L. Cohen, *J. Phys. C* **12**, 4409 (1979); G. Kerker, *ibid.* **13**, L189 (1980).

¹¹ S. Froyen, *Phys. Rev. B* **39**, 3168 (1989).

¹² J. J. Hopfield, *J. Phys. Chem. Solids* **15**, 97 (1960).

¹³ S. Froyen, D. M. Wood, and A. Zunger, *Phys. Rev. B* **37**, 6893 (1988).